Theory of fractional vortex escape in a long Josephson junction

K. Vogel,[1] W. P. Schleich,[1] T. Kato,[2] D. Koelle,[3] R. Kleiner,[3] and E. Goldobin[3,*]
[1]*Institut für Quantenphysik, Universität Ulm, D-89069 Ulm, Germany*
[2]*Institute for Solid State Physics, The University of Tokyo, Kashiwa, Chiba 277-8581, Japan*
[3]*Physikalisches Institut–Experimentalphysik II and Center for Collective Quantum Phenomena, Universität Tübingen, Auf der Morgenstelle 14, D-72076 Tübingen, Germany*

(Received 30 December 2008; revised manuscript received 27 July 2009; published 20 October 2009)

We consider a fractional Josephson vortex in an infinitely long 0-κ Josephson junction. A uniform bias current applied to the junction exerts a Lorentz force acting on a vortex. When the bias current becomes equal to the critical (or depinning) current, the Lorentz force tears away an integer fluxon and the junction switches to the resistive state. In the presence of thermal and quantum fluctuations this escape process takes place with finite probability already at subcritical values of the bias current. We analyze the escape of a fractional vortex by mapping the Josephson phase dynamics to the dynamics of a single particle in a metastable potential and derive the effective parameters of this potential. This allows us to predict the behavior of the escape rate as a function of the topological charge of the vortex.

DOI: 10.1103/PhysRevB.80.134515 PACS number(s): 74.50.+r, 75.45.+j, 85.25.Cp, 03.65.−w

I. INTRODUCTION

Josephson junctions (JJs) with a phase drop of π in the ground state [π JJs (Ref. 1)] are intensively investigated, as they promise important advantages for Josephson junction based electronics,[2,3] and, in particular, for JJ based qubits.[4–7] Nowadays several technologies allow to manufacture such junctions: JJs with ferromagnetic barrier,[8–10] quantum dot JJs[11–13] and nonequilibrium superconductor-normal metal-superconductor JJs.[14,15]

One can also fabricate 0-π long Josephson junctions (0-π LJJs),[16–20] i.e., LJJs some parts of which behave as 0 junctions and other parts as π junctions. The ground-state phase $\mu(x)$ in such junctions will have the value of 0 deep inside the 0 region, the value of π deep inside the π region and will continuously change from 0 to π in the λ_J vicinity of a 0-π boundary, where λ_J is the Josephson penetration depth. Such a bending of the phase results in the appearance of the magnetic field $\propto d\mu/dx$ localized in the λ_J vicinity of a 0-π boundary and the supercurrents $\pm\sin[\mu(x)]$ circulating around it, i.e., one deals with a Josephson vortex. The total magnetic flux localized at the 0-π boundary is equal to $\Phi_0/2$, where $\Phi_0 \approx 2.07\times 10^{-15}$ Wb is the magnetic flux quantum. Therefore, such a Josephson vortex is called a semifluxon.[21–23] If the Josephson phase $\mu(x)$ deep inside the π region is equal to $-\pi$ instead of π, one will have a localized magnetic flux equal to $-\Phi_0/2$ and a supercurrent of the vortex circulating counterclockwise (antisemifluxon). Both semifluxons and antisemifluxons were observed experimentally[24] and have been under extensive experimental and theoretical investigation during the last decade.[17,24–37]

It turns out that instead of a π discontinuity of the Josephson phase at a 0-π boundary one can artificially create any arbitrary κ discontinuity of the phase at any point of the LJJ, and the value of κ can be tuned electronically.[31] As a result, in the ground state two types of vortices with the topological charges $\varphi \equiv \mu(+\infty)-\mu(-\infty)=-\kappa$ and $\varphi=-\kappa+2\pi\,\mathrm{sgn}(\kappa)$ (we assume that $|\kappa|\leq 2\pi$, otherwise we have to deal with additional fluxons present in the system) can be formed.[33] Such φ vortices are generalizations of semifluxons and antisemifluxons discussed above. They are stable only if $|\varphi|\leq 2\pi$. For $\varphi\to 0$ one has a smooth transition to an empty LJJ, while for $|\varphi|\to 2\pi$ one gets the conventional integer (anti) fluxon, which is a freely moving soliton carrying the flux $\pm\Phi_0$. The possibility to change the value of κ and, therefore, φ electronically offers more control and tunability in experiments. For example, in a two antiferromagnetically arranged fractional vortex molecule having classically degenerate ground states $\uparrow\downarrow$ and $\downarrow\uparrow$, one can tune the height of the energy barrier separating these two states.

When one has a vortex with a topological charge φ (without loosing generality we assume $0\leq\varphi\leq 2\pi$) and applies a spatially uniform bias current through the LJJ, the bias current exerts a Lorentz force, which pushes the vortex along the junction. The direction of the force depends on the mutual polarity of the vortex and the bias current. The vortex exists just because it should compensate the phase discontinuity, and, therefore, it is pinned in the vicinity of the discontinuity, i.e., it may bend under the action of the Lorentz force, but does not move away. Nevertheless, when the Lorentz force becomes strong enough, it tears off a whole integer fluxon out of a φ vortex. The fluxon moves away along the junction, while a $\varphi-2\pi$ vortex is left at the discontinuity. Further time evolution leads to the switching of the 0-κ LJJ into the voltage state. This process was initially described for the case of a semifluxon ($\varphi=\pi$).[28] It takes place when the normalized bias current $\gamma=I/I_{c0}$ reaches the critical (depinning) current of[34,38]

$$\gamma_c(\varphi)=\left|\frac{\sin(\varphi/2)}{\varphi/2}\right|, \quad |\varphi|\leq 2\pi, \tag{1}$$

where I_{c0} is the "intrinsic" critical current, which corresponds to the measurable critical current if $\varphi=0$.

In the presence of quantum or thermal fluctuations, the escape process described above will take place with finite probability already at $\gamma<\gamma_c$. In this case, the phase $\mu(x)$ can tunnel through the barrier or escape over the barrier.

In this paper, we study the escape process of an arbitrary fractional Josephson vortex by mapping the Josephson phase dynamics to the dynamics of a fictitious particle in an effective one-dimensional metastable potential. This allows us to predict the escape rates as a function of the bias current and of the vortex topological charge $\wp$ in the thermal and quantum domains.

We consider arbitrary fractional vortices for the following reasons. First, since an electronically tunable κ and $\wp$ can be realized in experiment using a LJJ with injectors,[31,36] the predictions made here can be tested in the whole range of $\wp$. Of course, our results can be also used for LJJ technologies with fixed values of κ. Although, at the moment, only the 0-π JJs ($\kappa=\pm\pi$) are realized, e.g., *d*-wave superconductor-based LJJs[16–19] or LJJs with ferromagnetic barrier,[20] other fixed values of the phase jump are also possible, e.g., 0-$\pi/2$ JJ.[39,40] Our theory presented below covers all these cases in advance. Second, both in experiment and theory it is good to have a tuning parameter such as $\wp$, which allows to bring the system continuously to simple limiting cases such as an empty LJJ ($\wp=0$) or a single integer fluxon ($\wp=2\pi$). In this way one can see the connection with the known physics and even understand it better.

II. MODEL

For our calculations we use dimensionless quantities. Lengths are measured in units of the Josephson length λ_J, times are measured in units of ω_p^{-1}, where ω_p is the plasma frequency, energies are measured in units of $E_J\lambda_J$, where E_J is the Josephson energy per length, and currents are measured in units of the intrinsic critical current I_{c0} of the Josephson junction.

The dynamics of a fractional vortex in an infinitely long 0-κ Josephson junction with an applied bias current γ is then described by the sine-Gordon equation for the *continuous* phase[33] μ (dissipation is neglected)

$$\mu_{xx}(x,t) - \mu_{tt}(x,t) - \sin[\mu(x,t) + \kappa H(x)] = -\gamma, \tag{2}$$

where $H(x)$ is given by

$$H(x) = \begin{cases} 0 & \text{for } x < 0 \\ 1 & \text{for } x > 0. \end{cases} \tag{3}$$

This equation can be derived from the Lagrangian density

$$\mathcal{L} = \frac{1}{2}\left(\frac{\partial\mu}{\partial t}\right)^2 - \frac{1}{2}\left(\frac{\partial\mu}{\partial x}\right)^2 - U(\mu,x), \tag{4}$$

where the potential-energy density $U(\mu,x)$ is given by

$$U(\mu,x) = 1 - \cos[\mu + \kappa H(x)] - \gamma\mu. \tag{5}$$

The boundary conditions for $\mu(x,t)$ are

$$\mu_x(-\infty,t) = \mu_x(+\infty,t) = 0. \tag{6}$$

At $x=0$ the Josephson phase $\mu(x,t)$ and its derivative $\mu_x(x,t)$ are continuous, i.e.,

$$\mu(0^+,t) = \mu(0^-,t) = \mu(0,t), \tag{7a}$$

$$\mu_x(0^+,t) = \mu_x(0^-,t) = \mu_x(0,t). \tag{7b}$$

III. CLASSICAL DYNAMICS

As already discussed in the introduction, at a critical bias current γ_c, Eq. (1), the system switches between two types of solutions. Before we discuss this process in more detail, we briefly discuss a similar process in a pointlike Josephson junction.

Here the switching between two types of solutions at a critical bias current is usually visualized by a particle moving in a tilted washboard potential. If the bias current is below a critical value the potential has minima and stationary solutions, where the particle is trapped in one of the minima, are possible. If the bias current exceeds a critical value, the minima disappear and the particle is running down the washboard potential. The escape of a fractional vortex in a 0-κ long Josephson junction may be considered as a generalization of this process.

In the present paper we will often use only the vortex topological charge $\wp$, not specifying at which discontinuity it is pinned. In fact, it does not matter, as only the value of $\wp$ is important. For simplicity, in all derivations including κ we will assume that we deal with a direct vortex having $\wp=-\kappa$.

For $|\gamma| < \gamma_c(\wp)$ [see Eq. (1)], the stationary solutions of Eq. (2) are fractional vortices with a topological charge $\wp$ pinned at the vicinity of the phase discontinuity. They may bend under the action of the Lorentz force but do not move away. Figures 1(a) and 1(b) show the stationary solutions of Eq. (2) for $\gamma=0$ and $\gamma \lesssim \gamma_c$. For $\gamma=0$ the vortex is symmetric with respect to the phase discontinuity at $x=0$ whereas for $\gamma>0$ it bends under the influence of the Lorentz force.

When the Lorentz force becomes strong enough, i.e., when the bias current γ exceeds the critical value $\gamma_c(\wp)$, Eq. (1), the stationary solutions discussed above can not exist. Instead, a whole integer fluxon is torn away from the vortex with a topological charge $\wp$ and moves along the junction, while a vortex with a topological charge $\wp-2\pi$ is left at the phase discontinuity. The magnetic field dynamics is presented in Fig. 1(c). Further time evolution leads to the switching of the LJJ into the voltage state.[28]

For $\gamma=0$ the stationary solution of the sine-Gordon equation (2) corresponding to a $\wp$ vortex is given by[33]

$$\mu_0(x) = \begin{cases} 4\arctan\left[\tan\left(\dfrac{\wp}{8}\right)e^{+x}\right], & x < 0; \\ \wp - 4\arctan\left[\tan\left(\dfrac{\wp}{8}\right)e^{-x}\right], & x > 0. \end{cases} \tag{8}$$

For finite values of γ no analytical expressions are available. Therefore, we have solved Eq. (2) numerically.

If we include quantum or thermal fluctuations the switching between the two types of solutions discussed above will take place with finite probability before the bias current reaches its critical value. The main topic of the present paper is to calculate these quantum and thermal escape rates for fractional vortices.

Our calculations are based on eigenmodes of the stationary solution of the sine-Gordon equation (2). Therefore we now discuss the properties of the stationary solution and the eigenmodes of Eq. (2) before we derive an effective potential for the escape process.

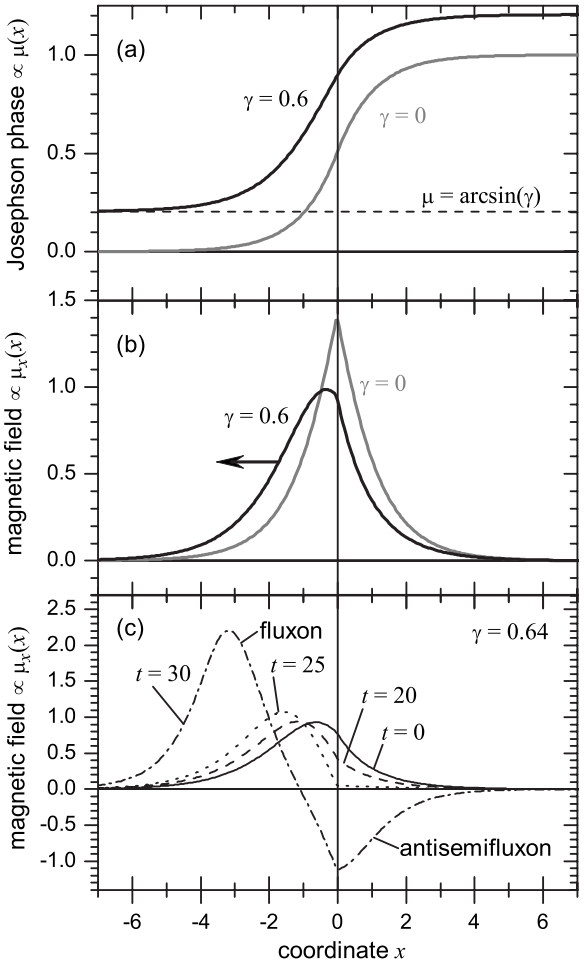

FIG. 1. (a) Phase profiles $\mu(x)$ and (b) magnetic field profiles $\mu_x(x)$ corresponding to the static solutions (vortex with a topological charge $\wp$ pinned at the phase discontinuity at $x=0$) of the sine-Gordon equation (2) with $\wp=\pi$ and $\gamma=0$ (gray), and $\gamma=0.6$ (black). Note, that $\gamma_c(\pi)=2/\pi\approx 0.635$, see Eq. (1). (c) Shows the depinning dynamics, i.e., the magnetic field profile $\mu_x(x)$ as a function of time after the bias current γ was abruptly increased from 0.63 (still static solution) to 0.64 (no static solution) at $t=0$. One can see a fluxon separating and moving to the left and an antisemifluxon left at the discontinuity.

IV. PROPERTIES OF THE STATIONARY SOLUTION

The stationary solution $\mu_0(x)$ of Eq. (2) follows from:

$$\mu_0''(x) - U'[\mu_0(x),x] = \mu_0''(x) - \sin[\mu_0(x) + \kappa H(x)] + \gamma = 0. \tag{9}$$

Without solving this equation we can derive some properties of $\mu_0(x)$ which will be useful for our calculations. Multiplying Eq. (9) with $\mu_0'(x)$ in the regions $x<0$ and $x>0$ leads to

$$-\frac{1}{2}[\mu_0'(x)]^2 + U[\mu_0(x),x] = \text{const.} \tag{10}$$

Using the boundary conditions (6) for the stationary solution and the abbreviations

$$\varphi_- = \mu_0(-\infty); \tag{11a}$$

$$\varphi_+ = \mu_0(+\infty) + \kappa; \tag{11b}$$

$$\varphi_0 = \mu_0(0) + \kappa/2, \tag{11c}$$

we obtain

$$\begin{aligned} x<0:\ &\frac{1}{2}[\mu_0'(x)]^2 \\ &= U[\mu_0(x),x] - U[\mu_0(-\infty),-\infty] \\ &= \cos\varphi_- - \cos[\mu_0(x)] + \gamma[\varphi_- - \mu_0(x)] \\ x>0:\ &\frac{1}{2}[\mu_0'(x)]^2 \\ &= U[\mu_0(x),x] - U[\mu_0(+\infty),+\infty] \\ &= \cos\varphi_+ - \cos[\mu_0(x)+\kappa] + \gamma[\varphi_+ - \mu_0(x) - \kappa]. \end{aligned} \tag{12}$$

These two equations allow us to express $\mu_0'(x)$ in terms of $\mu_0(x)$ and $\varphi_\pm$ [or $\mu_0(\pm\infty)$]. Furthermore, since $\mu_0(x)$ and $\mu_0'(x)$ are continuous at $x=0$, we have

$$\begin{aligned} &U[\mu_0(0),0^-] - U[\mu_0(-\infty),-\infty] \\ &\quad = U[\mu_0(0),0^+] - U[\mu_0(+\infty),+\infty] \end{aligned} \tag{13}$$

which we can rewrite in the form

$$\begin{aligned} &\cos\varphi_+ - \cos\varphi_- + \gamma(\varphi_+ - \varphi_- - \kappa) \\ &\quad = \cos[\varphi_0 + \kappa/2] - \cos[\varphi_0 - \kappa/2] \\ &\quad = -2\sin\frac{\kappa}{2}\sin\varphi_0. \end{aligned} \tag{14}$$

For $x\to\pm\infty$ the phase $\mu_0(x)$ approaches a constant value, which minimizes the potential-energy density $U[\mu_0(x),x]$, Eq. (5). From this condition we find

$$\sin\varphi_\pm = \gamma, \quad \cos\varphi_\pm > 0 \Rightarrow \varphi_\pm = \arcsin\gamma + 2n_\pm\pi,$$

$$\cos\varphi_\pm = \sqrt{1-\gamma^2}. \tag{15}$$

Using this result, Eq. (14) can be reduced to

$$\gamma(2n\pi - \kappa) = -2\sin\frac{\kappa}{2}\sin\varphi_0, \tag{16}$$

where $n=n_+-n_-$ is the number of fluxons already present in the system. Obviously, this condition cannot be fulfilled for arbitrary values of γ. At a critical value γ_c we will find $\sin\varphi_0=\pm 1$. For larger values of γ, Eq. (16) has no solution for φ_0, and the stationary solution $\mu_0(x)$ cannot exist. For $n=0$, i.e., $\varphi_+=\varphi_-$, we obtain the critical current given in Eq. (1).

V. EIGENMODES

The stability of the stationary solution $\mu_0(x)$ can be analyzed with the help of the eigenmodes of the sine-Gordon equation (2). To find these eigenmodes we insert the ansatz

$$\mu(x,t) = \mu_0(x) + \psi(x)e^{-i\omega t} \tag{17}$$

into the sine-Gordon equation (2) and linearize it, assuming $|\psi(x)| \ll 1$. Since $\mu_0(x)$ solves the stationary sine-Gordon equation, we obtain the Schrödinger equation

$$\begin{aligned} &-\psi_n''(x) + U''[\mu_0(x),x]\psi_n(x) \\ &\quad = -\psi_n''(x) + \cos[\mu_0(x) + \kappa H(x)]\psi_n(x) = \omega_n^2 \psi_n(x) \end{aligned} \tag{18}$$

for the eigenmodes $\psi_n(x)$, where the index n enumerates the eigenmodes. In this Schrödinger equation, the potential is determined by the stationary solution $\mu_0(x)$. Since the boundary conditions for $\mu(x,t)$ are already taken into account by the stationary solution $\mu_0(x)$, the boundary conditions for the eigenmodes $\psi_n(x)$ read

$$\psi_n'(-\infty) = \psi_n'(+\infty) = 0. \tag{19}$$

At $x=0$ the phase $\mu(x,t)$ and its derivative $\mu_x(x,t)$ are continuous, see Eq. (7). Since the stationary solution $\mu_0(x)$ and its derivative $\mu_0'(x)$ are continuous at $x=0$, $\psi_n(x)$ and $\psi_n'(x)$ have to be continuous at $x=0$ as well, i.e.,

$$\psi_n(0^+) = \psi_n(0^-) = \psi_n(0); \tag{20a}$$

$$\psi_n'(0^+) = \psi_n'(0^-) = \psi_n'(0). \tag{20b}$$

As long as all eigenvalues ω_n^2 of the Schrödinger equation (18) are positive, the stationary solution $\mu_0(x)$ is stable. As soon as one eigenvalue ω_n^2 becomes negative, the stationary solution $\mu_0(x)$ is unstable. Therefore, at the critical current $\gamma=\gamma_c$ the lowest eigenvalue, denoted by ω_0^2, becomes zero.

We now briefly show that at $\gamma=\gamma_c$ the lowest eigenmode $\psi_0(x)$ is the derivative of the stationary solution, i.e., $\psi_0(x) = C\mu_0'(x)$. By taking the derivative of the stationary sine-Gordon equation (9) in the regions $x<0$ and $x>0$ we find

$$-\frac{d^2}{dx^2}\mu_0'(x) + \cos[\mu_0(x) + \kappa H(x)]\mu_0'(x) = 0. \tag{21}$$

Therefore, we have found the formal solution $\psi_0(x) = C\mu_0'(x)$ of the Schrödinger equation (18) with an eigenvalue $\omega_0^2=0$.

The boundary conditions (19) and the matching conditions (20) for the eigenmodes introduce additional conditions for the stationary solution $\mu_0(x)$

$$\psi_0'(\pm\infty) = C\mu_0''(\pm\infty) = 0 \Rightarrow \mu_0''(\pm\infty) = 0, \tag{22a}$$

$$\psi_0'(0^+) = C\mu_0''(0^+) = \psi_0'(0^-) = C\mu_0''(0^-) \Rightarrow \mu_0''(0^+) = \mu_0''(0^-). \tag{22b}$$

Using the stationary sine-Gordon equation (9) and the abbreviations defined in Eq. (11), we can rewrite these conditions in the form

$$\sin\varphi_- = \sin\varphi_+ = \gamma, \tag{23a}$$

$$\sin(\varphi_0 - \kappa/2) = \sin(\varphi_0 + \kappa/2) \Rightarrow \sin\frac{\kappa}{2}\cos\varphi_0 = 0. \tag{23b}$$

The first condition is fulfilled for any value of γ, see Eq. (15), whereas the second condition is only true for $\gamma=\gamma_c$, where we have $\sin\varphi_0 = \pm 1$ and $\cos\varphi_0 = 0$, see the discussion after Eq. (16). Therefore, $\psi_0(x) = C\mu_0'(x)$ is only an eigenmode for $\gamma=\gamma_c$, see also Ref. 41.

VI. EFFECTIVE POTENTIAL

The phase $\mu(x,t)$ can be written in the form

$$\mu(x,t) = \mu_0(x) + \sum_n q_n(t)\psi_n(x). \tag{24}$$

By inserting this expansion into the Lagrangian density (4) and integrating over x we can derive a Lagrangian for the mode amplitudes $q_n(t)$, which describes the motion of a fictitious particle in many dimensions. For γ close to γ_c the eigenfrequency ω_0 approaches zero, whereas the other eigenfrequencies remain finite. Around the minimum at $q_n=0$ the potential will be "flat" in the direction of q_0 and "steep" along the other directions. Therefore, we expect that at low energies, a particle trapped in the minimum of the potential will move along q_0. Motivated by this simple picture, we only take into account the dynamics of the mode amplitude $q_0(t)$. To simplify the notation we denote the amplitude of the eigenmode $\psi_0(x)$ by $q(t)$.

The Lagrangian for $q(t)$ can be derived by inserting the ansatz

$$\mu(x,t) \approx \mu_0(x) + q(t)\psi_0(x) \tag{25}$$

into the Lagrangian density (4). Our simplified Lagrangian reads

$$\begin{aligned} L = \int_{-\infty}^{+\infty} \mathcal{L}dx &= \frac{1}{2}\dot{q}^2(t)\int_{-\infty}^{+\infty}\psi_0^2(x)dx \\ &- \frac{1}{2}\int_{-\infty}^{+\infty}[\mu_0'(x) + q(t)\psi_0'(x)]^2 dx \\ &- \int_{-\infty}^{+\infty} U[\mu_0(x) + q(t)\psi_0(x),x]dx, \end{aligned} \tag{26}$$

where $\mathcal{L}$ and U are defined in Eqs. (4) and (5). Since we want to describe the escape of a particle from a metastable potential we only take in to account terms up to third order in $q(t)$ and use the approximation

$$\begin{aligned} U[\mu_0(x) + q(t)\psi_0(x),x] \approx\ & U[\mu_0(x),x] + q(t)U'[\mu_0(x),x]\psi_0(x) \\ &+ \frac{1}{2}q^2(t)U''[\mu_0(x),x]\psi_0^2(x) \\ &+ \frac{1}{6}q^3(t)U'''[\mu_0(x),x]\psi_0^3(x). \end{aligned} \tag{27}$$

After omitting a constant term we obtain

$$L = \frac{1}{2}\dot{q}^2(t)\int_{-\infty}^{+\infty}\psi_0^2(x)dx - q(t)\int_{-\infty}^{+\infty}\{\mu_0'(x)\psi_0'(x) + U'[\mu_0(x),x]\psi_0(x)\}dx - \frac{1}{2}q^2(t)\int_{-\infty}^{+\infty}\{[\psi_0'(x)]^2 + U''[\mu_0(x),x]\psi_0^2(x)\}dx - \frac{1}{6}q^3(t)\int_{-\infty}^{+\infty}U'''[\mu_0(x),x]\psi_0^3(x)dx. \quad (28)$$

Performing two partial integrations and taking into account the boundary conditions for $\mu_0(x)$ and $\psi_0(x)$ leads to

$$L = \frac{1}{2}\dot{q}^2(t)\int_{-\infty}^{+\infty}\psi_0^2(x)dx - q(t)\int_{-\infty}^{+\infty}\{-\mu_0''(x) + U'[\mu_0(x),x]\}\psi_0(x)dx - \frac{1}{2}q^2(t)\int_{-\infty}^{+\infty}\{-\psi_0''(x) + U''[\mu_0(x),x]\psi_0(x)\}\psi_0(x)dx - \frac{1}{6}q^3(t)\int_{-\infty}^{+\infty}U'''[\mu_0(x),x]\psi_0^3(x)dx. \quad (29)$$

The linear term vanishes since $\mu_0(x)$ is the stationary solution of the stationary sine-Gordon equation (9). In the quadratic term we can use $-\psi_0''(x)+U''[\mu_0(x),x]\psi_0(x)=\omega_0^2\psi_0(x)$, see Eq. (18). Therefore, the Lagrangian can be written in the form

$$L = \frac{1}{2}M\dot{q}^2(t) - \frac{1}{2}M\omega_0^2q^2(t) - \frac{1}{6}Gq^3(t), \quad (30)$$

where M and G are given by

$$M = \int_{-\infty}^{+\infty}\psi_0^2(x)dx,$$

$$G = \int_{-\infty}^{+\infty}U'''[\mu_0(x),x]\psi_0^3(x)dx = -\int_{-\infty}^{+\infty}\sin[\mu_0(x)+\kappa H(x)]\psi_0^3(x)dx. \quad (31)$$

This Lagrangian describes the motion of a fictitious particle of mass M along *collective* coordinate q in the effective potential

$$V_{\mathrm{eff}}(q) = \frac{1}{2}M\omega_0^2q^2 + \frac{1}{6}Gq^3, \quad (32)$$

which can be characterized by the frequency ω_0 for small oscillations around the minimum at $q=0$ and a barrier height

$$\Delta V = \frac{2M^3\omega_0^6}{3G^2}. \quad (33)$$

These two parameters determine the escape rates in the thermal and in the quantum regime, see Sec. VIII. Note, that the frequency for small oscillations around the minimum and the eigenfrequency of the lowest eigenmode, calculated from Eq. (18), are the same.

The calculation of the present section leads to the following procedure to determine the frequency ω_0 and the barrier height ΔV. (i) For a given bias current $\gamma<\gamma_c$ we solve the stationary sine-Gordon equation (9) numerically and find the stationary solution $\mu_0(x)$. (ii) For this stationary solution $\mu_0(x)$ we solve the Schrödinger equation (18) numerically and find the eigenmode $\psi_0(x)$ and the corresponding eigenvalue ω_0^2. (iii) Using the eigenmode $\psi_0(x)$ we calculate M and G numerically using Eq. (31) to find the barrier height ΔV from Eq. (33).

VII. ANALYTICAL APPROXIMATIONS

A. Approximations for M and G

The approximations for M and G for γ close to γ_c are straightforward. Since M and G remain finite at $\gamma=\gamma_c$ we replace M and G by their values at $\gamma=\gamma_c$ and use the unnormalized eigenmode $\psi_0(x)=\mu_0'(x)$, i.e.,

$$M \approx \int_{-\infty}^{+\infty}[\mu_0'(x)]^2dx, \quad (34a)$$

$$G \approx -\int_{-\infty}^{+\infty}\sin[\mu_0(x)+\kappa H(x)][\mu_0'(x)]^3dx. \quad (34b)$$

These two integrals can be calculated analytically to a large extent. As shown in the Appendix, the expressions for M and G can be written in the form

$$M = \pm\sqrt{2}\int_{\varphi_-}^{\varphi_0-\kappa/2}\sqrt{\cos\varphi_- - \cos\varphi + \gamma_c(\varphi_- - \varphi)}d\varphi \pm \sqrt{2}\int_{\varphi_0+\kappa/2}^{\varphi_+}\sqrt{\cos\varphi_+ - \cos\varphi + \gamma_c(\varphi_+ - \varphi)}d\varphi \quad (35)$$

and

$$G = 2\sin\frac{\kappa}{2}\sin\varphi_0[\cos\varphi_+ + \cos\varphi_- + \gamma_c(\varphi_+ + \varphi_- - 2\varphi_0)], \quad (36)$$

where φ_+, φ_-, and φ_0 follow from the behavior of the stationary solution for $\gamma=\gamma_c$ at $x=\pm\infty$ and $x=0$, see Eq. (11). The upper sign for M applies to vortices with $\mu_0'(x)>0$, whereas the lower sign applies to vortices with $\mu_0'(x)<0$.

For our examples in Sec. IX we use vortices with

$$\mu_0(-\infty) = \arcsin\gamma, \quad (37a)$$

$$\mu_0(+\infty) = \arcsin\gamma + \wp \quad (37b)$$

to satisfy Eq. (15), i.e., direct vortices with $\wp=-\kappa$. In the limit $\gamma\to\gamma_c$ we therefore have $\varphi_+=\varphi_-=\arcsin\gamma_c=\varphi_c$ which

for positive bias currents implies $\varphi_0=\pi/2$. Moreover, $\mu_0'(x)$ is positive for $-2\pi<\kappa<0$ and negative for $0<\kappa<2\pi$. In this case the expressions (35) and (36) for M and G reduce to

$$M=\sqrt{2}\int_{(\pi-|\kappa|)/2}^{(\pi+|\kappa|)/2}\sqrt{\cos\varphi_c-\cos\varphi+\gamma_c(\varphi_c-\varphi)}d\varphi, \tag{38a}$$

$$G=4\sin\frac{\kappa}{2}[\cos\varphi_c+\gamma_c(\varphi_c-\pi/2)]. \tag{38b}$$

B. Approximations for ω_0 and ΔV

Since ω_0^2 vanishes for $\gamma\to\gamma_c$ we cannot use its value at γ_c. Instead we use the stationary solution $\mu_0(x)$ and the eigenmode $\psi_0(x)=\mu_0'(x)$ at $\gamma=\gamma_c$ to evaluate Lagrangian (29) for $\gamma<\gamma_c$. In this case, the quadratic term in Eq. (29) vanishes since $U''[\mu_0(x),x]$ does not depend on γ. The linear term, however, does not vanish since $\mu_0(x)$ is not the stationary solution for $\gamma<\gamma_c$. Here we have

$$-\mu_0''(x)+U'[\mu_0(x),x]=-\mu_0''(x)+\sin[\mu_0(x)+\kappa H(x)]-\gamma=\gamma_c-\gamma. \tag{39}$$

The remaining integral can easily be calculated and the approximate effective potential reads

$$V_{\text{eff}}(q)\approx\wp(\gamma_c-\gamma)q+\frac{1}{6}Gq^3, \tag{40}$$

where we have used

$$\int_{-\infty}^{+\infty}\psi_0(x)dx=\int_{-\infty}^{+\infty}\mu_0'(x)dx=\mu_0(+\infty)-\mu_0(-\infty)=\wp. \tag{41}$$

For this potential we find the frequency

$$\omega_0^{\text{cr}}=\left[\frac{2G\wp}{M^2}(\gamma-\gamma_c)\right]^{1/4} \tag{42}$$

for small oscillations around the minimum and the barrier height

$$\Delta V^{\text{cr}}=\frac{2}{3}|G|\left[\frac{2\wp}{G}(\gamma-\gamma_c)\right]^{3/2}=\frac{2M^3[\omega_0^{\text{cr}}]^6}{3G^2}. \tag{43}$$

The first expression for ΔV^{cr} does not depend on M whereas the second expression for ΔV^{cr} agrees with Eq. (33), except that now the approximate expressions for M, G, and ω_0 are used.

C. Pointlike Josephson junction

We would like to compare our results to the pointlike JJ in the following sense. At given $\wp$, in experiments one sees a certain value of I_c and can calculate the expected eigenfrequency, the barrier height and escape rates using a short JJ model which ignores phase discontinuities and details related to the internal structure of the solution. We compare these results with our results for a fractional vortex. To obtain the results from the pointlike JJ model we insert the values of γ and γ_c for a long 0-κ JJ into the well-known expressions for a pointlike JJ[42] and obtain

$$\Delta V^{\text{pt}}=2l\gamma_c\left[\sqrt{1-\left(\frac{\gamma}{\gamma_c}\right)^2}-\frac{\gamma}{\gamma_c}\arccos\frac{\gamma}{\gamma_c}\right] \tag{44}$$

and

$$\omega_0^{\text{pt}}=\sqrt{\gamma_c}\left[1-\left(\frac{\gamma}{\gamma_c}\right)^2\right]^{1/4}, \tag{45}$$

where l is the normalized length of the Josephson junction.

VIII. ESCAPE RATES

In Sec. VI we have found that we can map the escape of a fractional vortex to the escape of a particle from a one-dimensional cubic metastable potential which is characterized by the frequency ω_0 for small oscillations around the minimum and a barrier height ΔV. For such potentials approximate expressions for escape rates are available in the literature. As we use scaled quantities in the present paper we introduce the scaled temperature θ which measures temperatures in units of $E_J\lambda_J/k_B$ and the dimensionless parameter $\eta=\hbar\omega_p/(E_J\lambda_J)$ which plays the role of an effective $\hbar$.

In the classical regime, the escape of a particle from a metastable potential is due to thermal hopping. The escape rate (measured in units of ω_p) for such processes is given by Kramers' formula[43,44]

$$\Gamma_{\text{th}}=\rho\frac{\omega_0}{2\pi}e^{-\Delta V/\theta}, \tag{46}$$

where the prefactor ρ depends on the damping constant α of the system. For $\alpha/\omega_0\gtrsim 5\theta/(36\Delta V)$ it reads

$$\rho=\sqrt{1+\left(\frac{\alpha}{2\omega_0}\right)^2}-\frac{\alpha}{2\omega_0}. \tag{47}$$

If the damping constant α becomes too small, it has to be replaced by

$$\rho=\frac{36\alpha\Delta V}{5\theta\omega_0}. \tag{48}$$

In the quantum regime, the escape of a particle from a metastable potential is due to tunneling trough the energy barrier. In the semiclassical limit the decay rate of the ground state of a cubic metastable potential is given by[44–46]

$$\Gamma_{\text{qm}}=\sqrt{60}\omega_0\sqrt{\frac{18\Delta V}{5\pi\eta\omega_0}}\exp\left(-\frac{36}{5}\frac{\Delta V}{\eta\omega_0}\right). \tag{49}$$

According to Ref. 44 for Ohmic damping the crossover between thermal hopping and quantum tunneling occurs at the temperature

$$\theta^\star=\rho\frac{\eta\omega_0}{2\pi}, \tag{50}$$

where ρ is given by Eq. (47).

Before we present our results we have a closer look at Eqs. (46) and (49), in particular for small damping where we can use $\rho \approx 1$. For both equations, the escape rates should be exponentially small, i.e., the exponents $\Delta V/\theta$ and $36\Delta V/(5\eta\omega_0)$ should be large. Using Eq. (33) we find that Kramers' formula, Eq. (46), can be applied if ω_0 satisfies

$$\omega_0^6 \gg \frac{3G^2}{2M^3}\theta, \quad \omega_0^5 \gtrsim \frac{5G^2}{24M^3}\frac{\theta}{\alpha}, \quad \omega_0 \gg \alpha/2. \tag{51}$$

The last two conditions allow us to use $\rho \approx 1$. The semiclassical expression for the quantum mechanical escape rate (49) can be used for

$$\omega_0^5 \gg \frac{5G^2}{24M^3}\eta, \quad \omega_0 \gg \theta/\eta. \tag{52}$$

If the second condition is violated, the system will not be inthe quantum mechanical ground state, and we have to take into account the quantum decay from exited states which is not included in Eq. (49). For $\eta\omega_0 \ll \Delta V$ (many "bound" states in the metastable potential) we may thermally average the decay rates from the ground state and the excited states. For details see Ref. 44.

The conditions introduced so far define lower bounds for ω_0. On the other hand our simple model of a particle moving in a one-dimensional potential is only valid for γ close to γ_c where ω_0 becomes small. The main assumption we used to map the full problem to a one-dimensional problem was that ω_0^2 is much smaller than the other eigenvalues of the Schrödinger equation (18). Therefore, we have to require $\omega_0^2 \ll \omega_1^2$, where ω_1^2 is the eigenvalue of the first excited state of the Schrödinger equation (18), or the edge of the plasma band.

IX. RESULTS

Our numerical results are based on Eqs. (9) and (18). We solve these equations numerically for a symmetric junction with a length of $20\lambda_J$ to emulate an infinitely long JJ.

For our examples we use the following JJ parameters: critical current density $j_c = 100$ A/cm^2, specific capacitance $C = 4.2$ μF/cm^2, junction width $w = 1$ μm. This corresponds to $\omega_p = 2\pi \times 42.8$ GHz and $E_J\lambda_J = 78.4$ meV $= 909$ K. For these parameters, T and θ are related via $T = (E_J\lambda_J/k_B)\theta \approx 909\ \mathrm{K} \times \theta$, and the value of η is $\eta = 2.3 \times 10^{-3}$. Furthermore, we assume that we are in the semiclassical limit, where we can apply Eq. (49) and that we can use $\rho \approx 1$ in Eqs. (46) and (50).

A. Comparison of different methods

Before we present our results for escape rates, we first compare the approximations for ω_0 and ΔV presented in Sec. VII to the corresponding numerical values based on the single-mode approximation of Sec. VI. For this purpose we calculate the eigenfrequency and energy barrier using three approaches: (a) single-mode approximation for $\gamma < \gamma_c$, Eq. (18) for $n = 0$ and Eq. (33), denoted with nu as superscript; (b) approximation at $\gamma = \gamma_c$, Eqs. (42) and (43), denoted with cr as superscript; and (c) pointlike JJ formulas (44) and (45), denoted with pt as superscript.

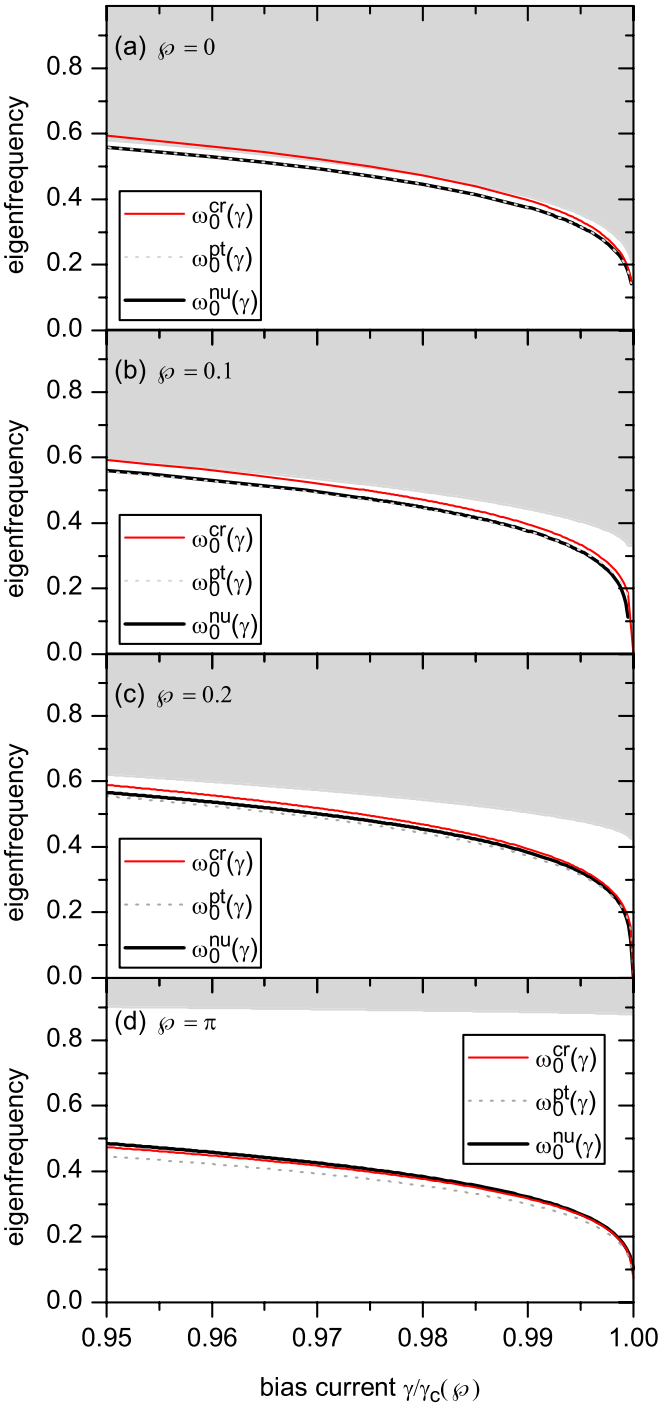

FIG. 2. (Color online) The frequencies ω_0^{cr}, ω_0^{pt}, and ω_0^{nu} as a function of the bias current γ for different values of $\wp$. The gray area indicates the plasma band, which was drawn by filling up the area above $\omega_1^{nu}(\gamma)$.

The eigenfrequencies are shown in Fig. 2. At $\wp = 0$ the eigenfrequency ω_0^{nu} coincides with ω_0^{pt}, while ω_0^{cr} provides a very reasonable approximation. At larger values of $\wp$ both ω_0^{pt} and ω_0^{cr} provide good approximations to ω_0^{nu}.

For our single-mode approximation to be valid, we have to make sure that the higher eigenfrequencies ω_n are much

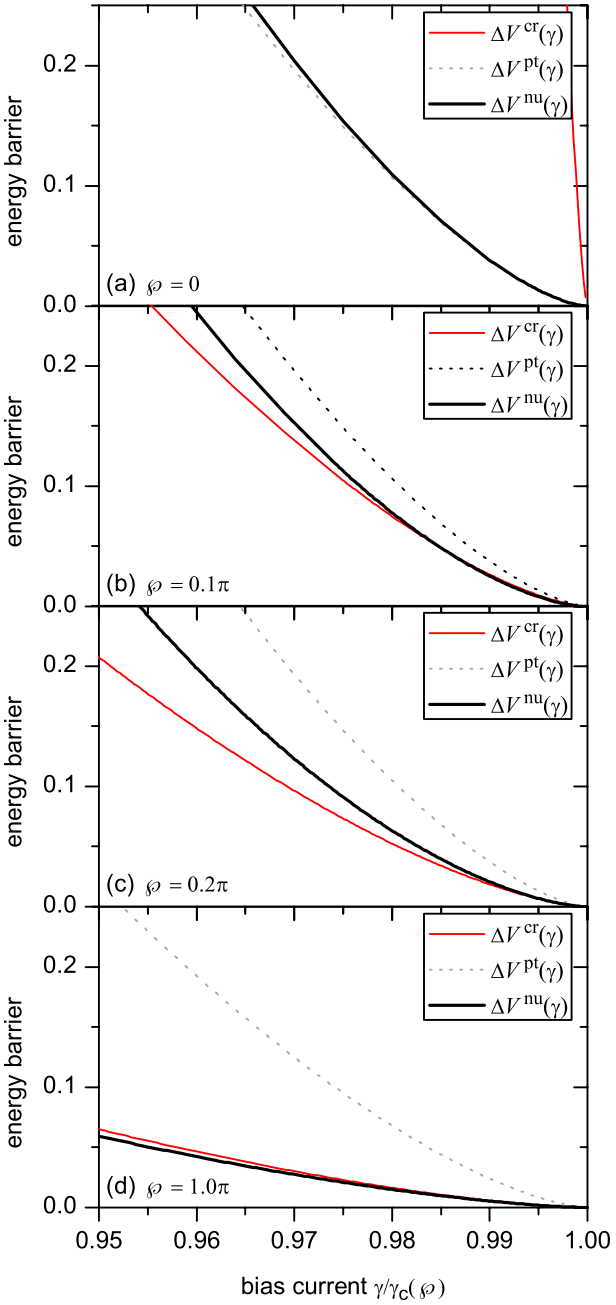

FIG. 3. (Color online) The energy barriers ΔV^{cr}, ΔV^{pt}, and ΔV^{nu} as a function of the bias current γ for different values of $\wp$. Note that ΔV^{cr} diverges for $\wp \to 0$. Therefore, we have plotted it for $\wp = 10^{-7}\pi$ in (a).

larger than ω_0. From Fig. 2 one can see that this is not the case for small values of $\wp$ where the eigenfrequency of a fractional vortex is close to the edge of the plasma band (shown in gray). Therefore, the *single-mode approximation fails to describe the escape process in a long JJ without discontinuities*. On the other hand, Fig. 2 shows the plasma band for an infinitely long JJ (approximated by $l=20\lambda_J$ here). For a JJ of finite normalized length l the plasma band consists of a set of discrete frequencies ω_n, where the spacing between ω_n is roughly inversely proportional to l. For moderate and especially for small values of l the difference between ω_0 and the other eigenfrequency becomes large, and the single-mode approximation works again even for $\wp \to 0$ (the pointlike JJ formula is valid).

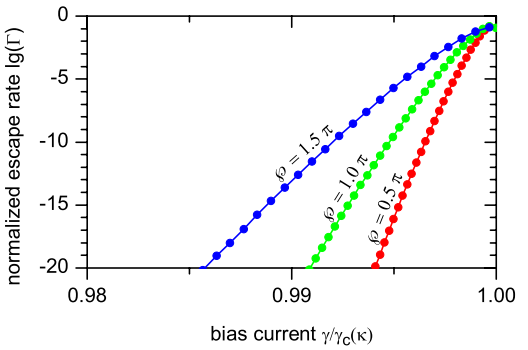

FIG. 4. (Color online) Quantum escape rates Γ_{qm} as a function of the bias current γ for different values of $\wp$.

The energy barrier calculated using different methods is shown in Fig. 3. For small values of $\wp$, ΔV^{pt} provides an excellent approximation to ΔV^{nu} as expected in this limit, while ΔV^{cr} quite overestimates the barrier. The latter happens because ΔV^{cr} is derived for an infinite LJJ, where at $\wp=0$ the phase string $\mu=$const escapes as a whole, thus having the barrier $\propto l=\infty$. Note, that we have chosen $l=20$ to emulate an infinitely long JJ as the vortex solution is localized on the length scale $1 \ll l$. However, for $\wp \to 0$ the phase becomes flat and looses its localization, so that both ΔV^{nu} and ΔV^{pt} become $\propto l$, whereas ΔV^{cr} does not depend on l. In any case, for $\wp \to 0$ the single (lowest) mode approximation does not work, so that one does not have to worry about the discrepancies in ΔV in this limit. For large values of $\wp$ ($\wp=\pi$) the situation reverses: ΔV^{cr} approximates ΔV^{nu} very well, while ΔV^{pt} gives overestimated values. The latter is expected as it is easier to activate a bent phase string starting the activation from some point than to move a flat string simultaneously over the barrier. It seems that starting from $\wp \sim 0.2\pi$ the values of ΔV^{cr} provide good approximations to ΔV^{nu}.

B. Quantum tunneling

We use the numerically calculated values for the eigenfrequency ω_0^{nu} and barrier height ΔV^{nu} and apply the semiclas-

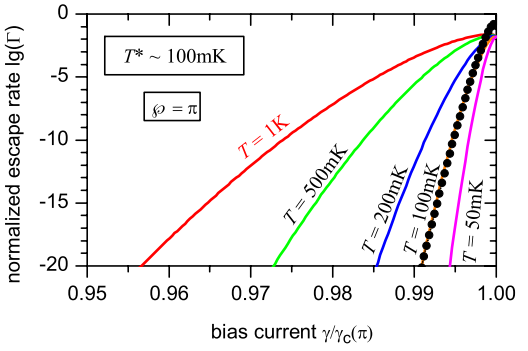

FIG. 5. (Color online) Thermal escape rates Γ_{th} as a function of the bias current γ for different temperatures. Dots represent the quantum escape rate Γ_{qm}. All escape rates are calculated for $\wp=\pi$.

sical formula (49) to these values to calculate quantum tunneling rates. The results are shown in Fig. 4. It turns out that the escape rate is larger, i.e., the vortex escapes easier, for larger values of $\wp$. This result is qualitatively understandable because for $\wp \to 0$ the escape process reminds more and more the escape of the flat string from the metastable minimum and should scale with the JJ length.

C. Thermal vs quantum escape

We use the numerically calculated values for the eigenfrequency ω_0^{nu} and barrier height ΔV^{nu} and apply Eq. (46) with $\rho=1$ and Eq. (49) to calculate escape rates at different temperatures T, as shown in Fig. 5 for $\wp=\pi$. The dots represent the quantum escape rate. We remind that these rates were obtained using the Eqs. (46) and (49) that are not valid very close to $\gamma_c(\wp)$, since in this case the escape rates are not exponentially small. Estimations using Eqs. (51) and (52) show that expression (46) at $T=100$ mK and expression (49) become invalid for $\gamma > 0.999\gamma_c(\pi)$. One can see that for $T=100$ mK the two escape rates agree very well for γ not very close to γ_c. We may therefore define a crossover temperature $T^\star \approx 100$ mK—independent of γ in the range of validity of Eqs. (46) and (49).

On the other hand, for the parameters used above Eq. (50) with $\rho=1$ and $\gamma=0$ gives $T^\star \approx 330$ mK. According to Fig. 2(d) in the region of interest the eigenfrequency $\omega_0(\pi,\gamma)$ is about three times smaller than $\omega_0(\wp,0)$. Thus Eq. (50) predicts $T^* \approx 110$ mK in this region.

X. CONCLUSIONS

We have investigated the thermal and quantum escape of an arbitrary fractional Josephson vortex close to its depinning current in an infinitely long Josephson junction. By using a single (lowest) mode approximation, we have mapped the dynamics of an infinite dimensional system to the problem of a pointlike particle escaping from a 1D metastable cubic potential. For small topological charge, the single-mode approximation fails because the lowest eigenmode is not well separated from the rest of the excitation spectrum. Thus, the lowest mode approximation cannot be used to describe the escape in a conventional long JJ ($\wp=0$).

In the region of validity of the single-mode approximation we have calculated the eigenfrequency and the barrier height numerically and analytically close to the depinning current. Then we have used Kramers' formula and a semiclassical expression for thermal and quantum escape rates, respectively, to compare escape rates of vortices with different topological charges and find the thermal-to-quantum crossover temperature. We have found that vortices with a larger topological charge escape easier. For typical experimental parameters the crossover temperature lays in the range of 100 mK as for many other JJ systems. These results can be directly compared to experiments. For example, recently[47] the thermal escape of a fractional vortex in a LJJ with an artificially created discontinuity has been studied as a function of $\wp$ and a good agreement between the experimental data and the theory presented here was found in the limit of large junction length and vortex topological charge. The macroscopic quantum tunneling experiments on this system are now in progress in the Tübingen group.

ACKNOWLEDGMENT

Financial support by the DFG (Project No. SFB/TRR-21) is gratefully acknowledged.

APPENDIX: INTEGRALS

In this appendix we evaluate the integrals for M and G. The calculations of this appendix are based on the unnormalized eigenmode $\psi_0(x)=\mu_0'(x)$ which is only valid for $\gamma=\gamma_c$. Furthermore, we use the abbreviations φ_+, φ_-, and φ_0 as defined in Eq. (11).

With the help of Eq. (12) the integral in the definition of G can be evaluated analytically for $\gamma=\gamma_c$

$$
\begin{aligned}
G &= -\int_{-\infty}^{+\infty} \sin[\mu_0(x)+\kappa H(x)][\mu_0'(x)]^3 dx = -\int_{-\infty}^{0} \sin[\mu_0(x)][\mu_0'(x)]^3 dx - \int_{0}^{\infty} \sin[\mu_0(x)+\kappa][\mu_0'(x)]^3 dx \\
&= -2\int_{\mu_0(-\infty)}^{\mu_0(0)} \sin\varphi[\cos\varphi_- - \cos\varphi + \gamma_c(\varphi_- - \varphi)]d\varphi - 2\int_{\mu_0(0)}^{\mu_0(+\infty)} \sin(\varphi+\kappa)[\cos\varphi_+ - \cos(\varphi+\kappa) + \gamma_c(\varphi_+ - \varphi - \kappa)]d\varphi \\
&= -2\int_{\varphi_-}^{\varphi_0-\kappa/2} \sin\varphi[\cos\varphi_- - \cos\varphi + \gamma_c(\varphi_- - \varphi)]d\varphi - 2\int_{\varphi_0+\kappa/2}^{\varphi_+} \sin\varphi[\cos\varphi_+ - \cos\varphi + \gamma_c(\varphi_+ - \varphi)]d\varphi \\
&= -2\left[\frac{1}{2}\cos^2\varphi - \cos\varphi_-\cos\varphi - \gamma_c\sin\varphi - \gamma_c(\varphi_- - \varphi)\cos\varphi\right]_{\varphi_-}^{\varphi_0-\kappa/2} \\
&\quad -2\left[\frac{1}{2}\cos^2\varphi - \cos\varphi_+\cos\varphi - \gamma_c\sin\varphi - \gamma_c(\varphi_+ - \varphi)\cos\varphi\right]_{\varphi_0+\kappa/2}^{\varphi_+} \\
&= -\cos^2(\varphi_0-\kappa/2) - 2\gamma_c\sin(\varphi_0-\kappa/2) + 2\cos(\varphi_0-\kappa/2)[\cos\varphi_- + \gamma_c(\varphi_- - \varphi_0 + \kappa/2)] - \cos^2\varphi_- + \cos^2\varphi_+ \\
&\quad + 2\gamma_c(\sin\varphi_- - \sin\varphi_+) + \cos^2(\varphi_0+\kappa/2) - 2\gamma_c\sin(\varphi_0+\kappa/2) - 2\cos(\varphi_0+\kappa/2)[\cos\varphi_+ + \gamma_c(\varphi_+ - \varphi_0 - \kappa/2)].
\end{aligned}
\tag{A1}
$$

Using Eqs. (14) and (23)we finally arrive at

$$G = 2\sin\frac{\kappa}{2}\sin\varphi_0[\cos\varphi_+ + \cos\varphi_- + \gamma_c(\varphi_+ + \varphi_- - 2\varphi_0)]. \tag{A2}$$

In a similar way we can derive an expression for M. With the help of Eq. (12) we obtain

$$\begin{aligned} M &= \int_{-\infty}^{+\infty}[\mu_0'(x)]^2dx = \int_{-\infty}^{0}[\mu_0'(x)]^2dx + \int_{0}^{+\infty}[\mu_0'(x)]^2dx \\ &= \pm\sqrt{2}\int_{\mu_0(-\infty)}^{\mu_0(0)}\sqrt{\cos\varphi_- - \cos\varphi + \gamma_c(\varphi_- - \varphi)}d\varphi \pm \sqrt{2}\int_{\mu_0(0)}^{\mu_0(+\infty)}\sqrt{\cos\varphi_+ - \cos(\varphi+\kappa) + \gamma_c(\varphi_+ - \varphi - \kappa)}d\varphi \\ &= \pm\sqrt{2}\int_{\varphi_-}^{\varphi_0-\kappa/2}\sqrt{\cos\varphi_- - \cos\varphi + \gamma_c(\varphi_- - \varphi)}d\varphi \pm \sqrt{2}\int_{\varphi_0+\kappa/2}^{\varphi_+}\sqrt{\cos\varphi_+ - \cos\varphi + \gamma_c(\varphi_+ - \varphi)}d\varphi. \end{aligned} \tag{A3}$$

The upper sign applies to vortices with $\mu_0'(x) > 0$ whereas the lower sign applies to vortices with $\mu_0'(x) < 0$.

*gold@uni-tuebingen.de

[1] L. N. Bulaevskiĭ, V. V. Kuziĭ, and A. A. Sobyanin, JETP Lett. **25**, 290 (1977) Pis'ma Zh. Eksp. Teor. Fiz. **25**, 314 (1977).
[2] E. Terzioglu, D. Gupta, and M. R. Beasley, IEEE Trans. Appl. Supercond. **7**, 3642 (1997).
[3] E. Terzioglu and M. R. Beasley, IEEE Trans. Appl. Supercond. **8**, 48 (1998).
[4] L. B. Ioffe, V. B. Geshkenbein, M. V. Feigel'man, A. L. Fauchère, and G. Blatter, Nature (London) **398**, 679 (1999).
[5] G. Blatter, V. B. Geshkenbein, and L. B. Ioffe, Phys. Rev. B **63**, 174511 (2001).
[6] T. Yamashita, K. Tanikawa, S. Takahashi, and S. Maekawa, Phys. Rev. Lett. **95**, 097001 (2005).
[7] T. Yamashita, S. Takahashi, and S. Maekawa, Appl. Phys. Lett. **88**, 132501 (2006).
[8] V. V. Ryazanov, V. A. Oboznov, A. Y. Rusanov, A. V. Veretennikov, A. A. Golubov, and J. Aarts, Phys. Rev. Lett. **86**, 2427 (2001).
[9] T. Kontos, M. Aprili, J. Lesueur, F. Genêt, B. Stephanidis, and R. Boursier, Phys. Rev. Lett. **89**, 137007 (2002).
[10] M. Weides, M. Kemmler, E. Goldobin, D. Koelle, R. Kleiner, and H. Kohlstedt, Appl. Phys. Lett. **89**, 122511 (2006).
[11] J. A. van Dam, Y. V. Nazarov, E. P. A. M. Bakkers, S. De Franceschi, and L. P. Kouwenhoven, Nature (London) **442**, 667 (2006).
[12] J.-P. Cleuziou, W. Wernsdorfer, V. Bouchiat, T. Ondarcuhu, and M. Monthioux, Nature Nanotech. **1**, 53 (2006).
[13] H. Jorgensen, T. Novotny, K. Grove-Rasmussen, K. Flensberg, and P. Lindelof, Nano Lett. **7**, 2441 (2007).
[14] J. J. A. Baselmans, A. F. Morpurgo, B. J. V. Wees, and T. M. Klapwijk, Nature (London) **397**, 43 (1999).
[15] J. Huang, F. Pierre, T. T. Heikkilä, F. K. Wilhelm, and N. O. Birge, Phys. Rev. B **66**, 020507(R) (2002).
[16] C. C. Tsuei and J. R. Kirtley, Rev. Mod. Phys. **72**, 969 (2000).
[17] J. R. Kirtley, C. C. Tsuei, M. Rupp, J. Z. Sun, L. S. Yu-Jahnes, A. Gupta, M. B. Ketchen, K. A. Moler, and M. Bhushan, Phys. Rev. Lett. **76**, 1336 (1996).
[18] F. Lombardi, F. Tafuri, F. Ricci, F. Miletto Granozio, A. Barone, G. Testa, E. Sarnelli, J. R. Kirtley, and C. C. Tsuei, Phys. Rev. Lett. **89**, 207001 (2002).
[19] H.-J. H. Smilde, Ariando D. H. A. Blank G. J. Gerritsma H. Hilgenkamp, and H. Rogalla, Phys. Rev. Lett. **88**, 057004 (2002).
[20] M. Weides, M. Kemmler, H. Kohlstedt, R. Waser, D. Koelle, R. Kleiner, and E. Goldobin, Phys. Rev. Lett. **97**, 247001 (2006).
[21] L. N. Bulaevskii, V. V. Kuzii, and A. A. Sobyanin, Solid State Commun. **25**, 1053 (1978).
[22] E. Goldobin, D. Koelle, and R. Kleiner, Phys. Rev. B **66**, 100508(R) (2002).
[23] J. H. Xu, J. H. Miller, and C. S. Ting, Phys. Rev. B **51**, 11958 (1995).
[24] H. Hilgenkamp, Ariando H.-J. H. Smilde D. H. A. Blank G. Rijnders H. Rogalla J. R. Kirtley, and C. C. Tsuei, Nature (London) **422**, 50 (2003).
[25] V. G. Kogan, J. R. Clem, and J. R. Kirtley, Phys. Rev. B **61**, 9122 (2000).
[26] J. R. Kirtley, C. C. Tsuei, and K. A. Moler, Science **285**, 1373 (1999).
[27] J. R. Kirtley, K. A. Moler, and D. J. Scalapino, Phys. Rev. B **56**, 886 (1997).
[28] E. Goldobin, D. Koelle, and R. Kleiner, Phys. Rev. B **67**, 224515 (2003).
[29] N. Stefanakis, Phys. Rev. B **66**, 214524 (2002).
[30] A. Zenchuk and E. Goldobin, Phys. Rev. B **69**, 024515 (2004).
[31] E. Goldobin, A. Sterck, T. Gaber, D. Koelle, and R. Kleiner, Phys. Rev. Lett. **92**, 057005 (2004).
[32] H. Susanto, S. A. van Gils, T. P. P. Visser, Ariando H.-J. H. Smilde, and H. Hilgenkamp, Phys. Rev. B **68**, 104501 (2003).
[33] E. Goldobin, D. Koelle, and R. Kleiner, Phys. Rev. B **70**, 174519 (2004).
[34] E. Goldobin, N. Stefanakis, D. Koelle, and R. Kleiner, Phys. Rev. B **70**, 094520 (2004).
[35] J. R. Kirtley, C. C. Tsuei, Ariando, H. J. H. Smilde, and H. Hilgenkamp, Phys. Rev. B **72**, 214521 (2005).
[36] K. Buckenmaier, T. Gaber, M. Siegel, D. Koelle, R. Kleiner, and E. Goldobin, Phys. Rev. Lett. **98**, 117006 (2007).
[37] C. Nappi, E. Sarnelli, M. Adamo, and M. A. Navacerrada, Phys. Rev. B **74**, 144504 (2006).
[38] B. A. Malomed and A. V. Ustinov, Phys. Rev. B **69**, 064502 (2004).

[39] A. Y. Zyuzin, B. Spivak, and M. Hruška, Europhys. Lett. **62**, 97 (2003).
[40] N. Stefanakis, arXiv:cond-mat/0208473 (unpublished).
[41] T. Kato and M. Imada, J. Phys. Soc. Jpn. **66**, 1445 (1997).
[42] A. Wallraff, A. Lukashenko, C. Coqui, A. Kemp, T. Duty, and A. V. Ustinov, Rev. Sci. Instrum. **74**, 3740 (2003).
[43] P. Hänggi, P. Talkner, and M. Borkovec, Rev. Mod. Phys. **62**, 251 (1990).
[44] U. Weiss, *Dissipative Quantum Systems* (World Scientific, Singapore, 1999).
[45] S. Coleman, Phys. Rev. D **15**, 2929 (1977).
[46] A. O. Caldeira and A. J. Leggett, Ann. Phys. **149**, 374 (1983).
[47] U. Kienzle, T. Gaber, K. Buckenmaier, K. Ilin, M. Siegel, D. Koelle, R. Kleiner, and E. Goldobin, Phys. Rev. B **80**, 014504 (2009).